03,04,10,16

Control of the fundamental absorption edge of GeO_x thin films by thermal annealing

© K.N. Astankova[1], N.A. Kislukhin[1,2], A.D. Samus[3], A.A. Matsynin[3,4], S.V. Komogortsev[3,4], I.A. Azarov[1,5], V.A. Volodin[1,5]

[1] Rzhanov Institute of Semiconductor Physics, Siberian Branch, Russian Academy of Sciences, Novosibirsk, Russia
[2] Novosibirsk State Technical University, Novosibirsk, Russia
[3] Siberian State University of Science and Technology, Krasnoyarsk, Russia
[4] Kirensky Institute of Physics, Federal Research Center KSC SB, Russian Academy of Sciences, Krasnoyarsk, Russia
[5] Novosibirsk State University, Novosibirsk, Russia

E-mail: astankova-kn@isp.nsc.ru

Received February 12, 2026
Revised February 18, 2026
Accepted February 18, 2026

This paper presents the results on the modification of the optical properties of GeO_x thin films subjected to thermal annealing in the temperature range of 280−400 °C in air. The GeO_x films were deposited by thermal evaporation of germanium monoxide granules in vacuum and subsequent vapor condensation onto unheated glass substrates. Raman spectroscopy data reveal that annealing the germanium monoxide films up to 280 °C leads to the formation of amorphous Ge nanoparticles, while heating to 380 °C initiates their crystallization. From the measured transmittance and reflectance spectra of the GeO_x thin films before and after annealing, the dispersion curves of the refractive and absorption indices were calculated. Furthermore, analysis of the spectral dependence of the absorption coefficient in Tauc coordinates allowed us to determine the optical band gap of the GeO_x films. It was found that by varying the annealing temperature, the fundamental absorption edge of the GeO_x thin films can be effectively tuned.

Keywords: germanium monoxide, Raman spectroscopy, transmission and reflection spectroscopy, Tauc model, fundamental absorption edge.

DOI: 10.61011/PSS.2026.02.63380.8833

1. Introduction

Germanium oxides are widely used in practice for manufacture of the infrared transparent lenses, waveguides, photodetectors and glasses, as these oxides are featuring a beneficial combination of optical and mechanical characteristics [1,2]. In addition to crystalline and amorphous modifications of germanium dioxide in the solid state, amorphous germanium monoxide is also known. Some studies show that GeO_x may be well used in the anti-reflective coatings in solar cells [3], as well as part of the multilayer interference filters [4,5]. The effect of photo-induced variations in the refractive index and thickness was found in GeO_x films (Nazarov et al.), which makes it possible to obtain holographic gratings on their basis [6].

Of particular interest is the metastability of germanium monoxide. Films of amorphous germanium monoxide, when heated above 200 °C, undergo a disproportionation in reaction $2GeO_x \rightarrow (1 - x/2)Ge + x/2GeO_2$. Germanium clusters released in the oxide matrix can be electroactive, acting as deep traps for the charge carriers. Due to this, photo- and cathodoluminescence signals at room temperature in the visible and IR ranges can occur in GeO_x films after annealing [7,8]. By heating, it is possible to control the concentration, size, and phase of Ge clusters in GeO_x films (the depth of disproportionation). Such structural modifications should lead to a change in their optical characteristics. This work is focused on studying the evolution of optical transmission and reflection spectra in thin GeO_x films on glass during annealing, calculating their optical constants using modeling, and determining the edge of intrinsic absorption using Tauc model.

2. Experimental procedure

Germanium monoxide films were obtained by thermal sublimation in vacuum ($\sim 10^{-3}$ Pa) of GeO granules heated in a conical crucible made of tungsten wire to a temperature

of ~ 2400 K for 1.5 min [9]. The substrates were placed on the stage right beneath the evaporator at a distance of 9 cm. The cover glasses (Minimed) with a size of $25\times25\times0.17$ mm, which were ultrasonic cleaned in soap solution and hydrogen peroxide, served as substrates for deposition. The obtained GeO_x films were $\sim 150-200$ nm thick. According to X-ray photoelectron spectroscopy data, the stoichiometric parameter x in the studied GeO_x films was 1.04 [9].

The samples with GeO_x films were annealed in the temperature range $280-400\,^\circ$C for 2 min in air. The heating was carried out by applying a controlled alternating voltage to a ceramic heater. An aluminum plate was placed on top of the heater, on which the samples were annealed.

Raman spectra (RS) were recorded using a T64000 Horiba Jobin Yvon spectrometer at room temperature in a backscattering geometry. The 514.5 nm optical fiber laser was used as the source of the exciting radiation. The spectral resolution was at least $2\,cm^{-1}$. The diameter of the laser spot on the surface of the sample was $\sim 30\,\mu$m, and the beam power was 1 mW. No any significant local heating of the sample under the laser spot occurred and no disproportionation of GeO_x films during the measurement process was observed. The transmittance spectra of GeO_x films were registered using spectrophotometer SF-56 within the wavelengths from 0.19 to $1.1\,\mu$m with a step of $0.001\,\mu$m. Spectral resolution was $0.002\,\mu$m. To register the specular reflection spectra, PZO-9 appliance with the light incidence angle to normal 9° was used. A polished Si plate served as a reference mirror. The measured spectrum was normalized to the reflection spectrum of the reference mirror. The approximation of the experimental transmittance and reflection spectra of GeO_x films and the analysis of the real and imaginary parts of the refractive index were carried out using software No. 2022668094 of 04.10.2022: Egorov D.A., Azarov I.A., Volodin V.A. „Modeling of transmittance and reflection spectra of layered structures on a thick substrate allowing for the intra-layer interference".

3. Results and discussion

Figure 1 shows the RS spectra of GeO_x films before and after a series of annealing in different temperatures. No any singularities were found on the glass in RS spectrum of the initial GeO_x film (Figure 1, spectrum *1*). After the film had been annealed at $T = 280\,^\circ$C for 2 minutes a weak wide band near $275-280\,cm^{-1}$ appeared in the spectrum. There is no any translational symmetry in amorphous materials and, consequently, the quasi-momentum conservation law is not fulfilled, therefore, the Raman spectrum is determined by the effective (adjusted for Bose-Einstein factor) density of vibrational states. As a result, RS spectrum of amorphous germanium contains a band corresponding to the maximum density of states at frequencies $275-280\,cm^{-1}$, which is associated with inelastic light scattering by local TO-shaped

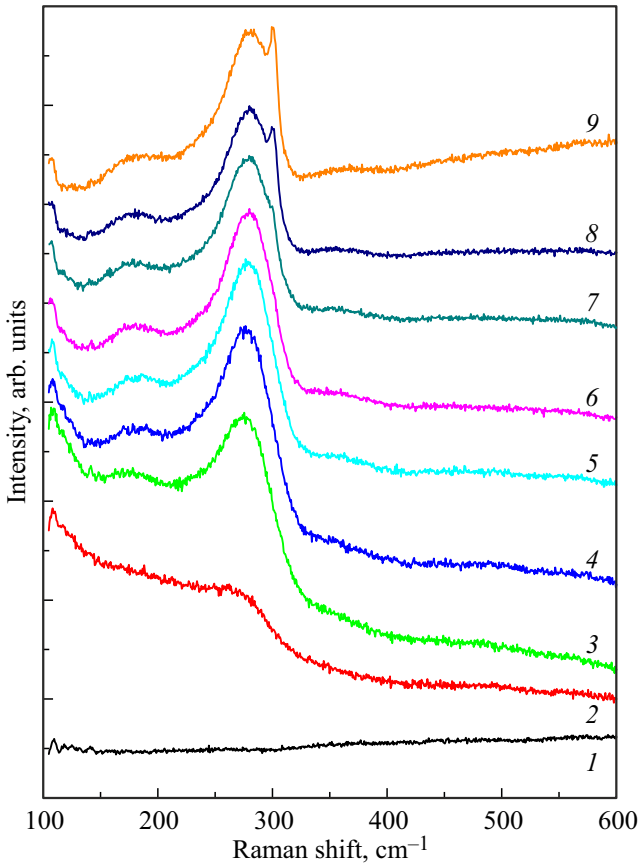

Figure 1. RS spectra of GeO_x films before (*1*) and after a series of 2 min annealings at a temperature of T, °C: *2* — 280, *3* — 300, *4* — 320, *5* — 340, *6* — 360, *7* — 380, *8* — 390, *9* — 400.

oscillations of Ge–Ge bonds (Figure 1, spectrum *2*) [10]. Thus, GeO film$_x$ is transformed into a composite system with Ge nanoclusters in a germanium oxide matrix at the beginning of disproportionation. There is also a background in the spectrum *2* that increases in the low frequency range. This is probably due to the wide bosonic peak, which is often present in RS spectra of glassy materials at frequencies $< 100\,cm^{-1}$ [11,12]. The annealing of GeO_x film at higher temperatures lead to emergence in RS spectrum a singularity (shoulder) near $180\,cm^{-1}$ related to the inelastic light scattering on LO-like vibrations of Ge–Ge bonds (Figure 1, spectrum *3*). The intensity of this band is much lower than the intensity of the band at $275-280\,cm^{-1}$, so it appears when RS intensity becomes noticeably high from the clusters of amorphous germanium. At the same time, the intensity of main RS band grows near $280\,cm^{-1}$, as the depth of disproportionation of GeO_x film rises with increasing annealing temperature (higher amount of released germanium). It should be noted that annealing of GeO_x films at temperatures of $380-400\,^\circ$C during 2 min results in a partial crystallization of Ge clusters which is evidenced by an emerged shoulder of $300.2\,cm^{-1}$ (Figure 1, spectrum *7*) and narrow peaks near $301\,cm^{-1}$ (Figure 1, spectra *8* and *9*). In crystalline germanium, the quasi-

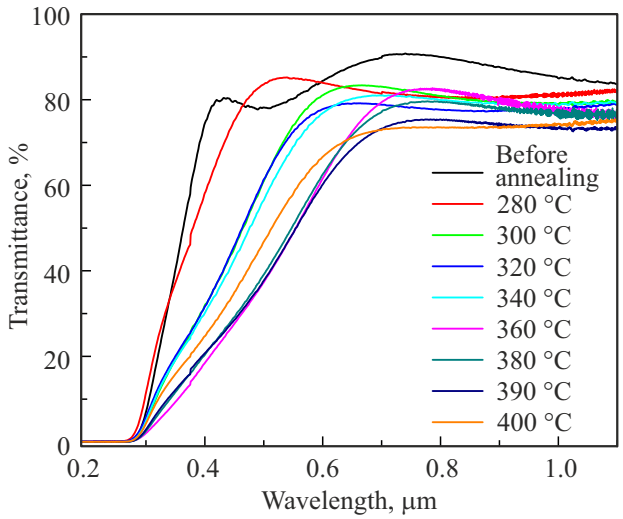

Figure 2. Transmittance spectra of GeO_x films before and after a series of 2 min annealings.

momentum conservation law is fulfilled, and since the photon momentum is very small, photons are inelastic scattered only by the long-wavelength phonons. The frequency of these phonons are $\sim 301.5\,cm^{-1}$ [13]. The frequency shift of phonons is due to their localization in Ge nanocrystals. Using the improved model of phonon localization in Ge nanocrystals [14], it can be determined from the position of RS spectrum narrow peak that their average diameter is $\sim 6-7$ nm (after annealing of GeO_x film at temperatures of 380 °C) and $\sim 9-10$ nm (at annealing temperatures of 390 and 400 °C). The onset temperature (T_c) of germanium clusters crystallization in the studied GeO_x films (380 °C) turned out to be much lower than T_c in GeO_x films with another composition (500–550 °C) [15–17]. This effect was first observed during annealing of $GeO_{1.07}$ films with a thickness of ~ 15 nm [18]. This effect is still unclear and is the subject of further investigations.

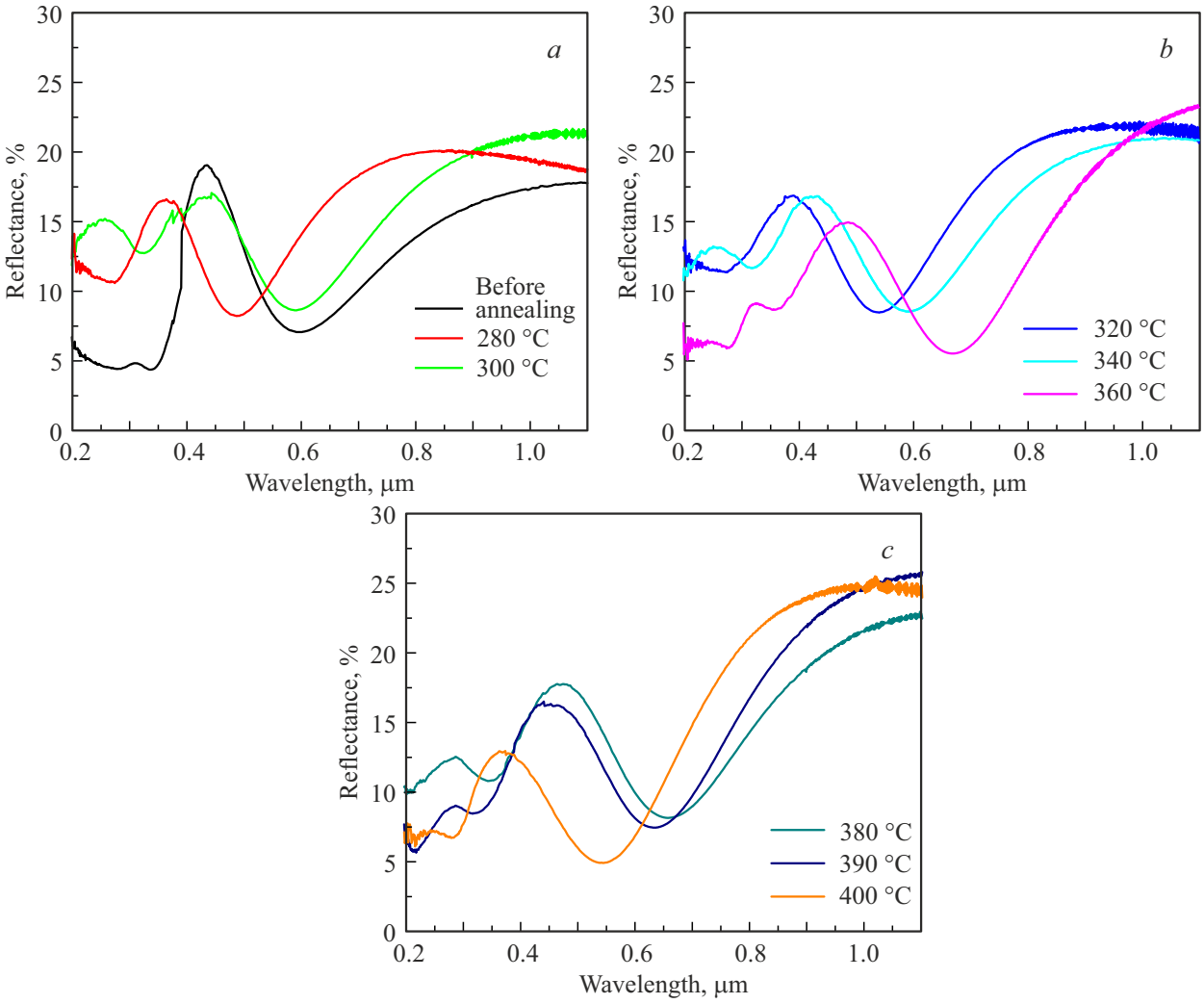

Figure 3. Reflection spectra of GeO_x films before and after a series of 2 min annealings.

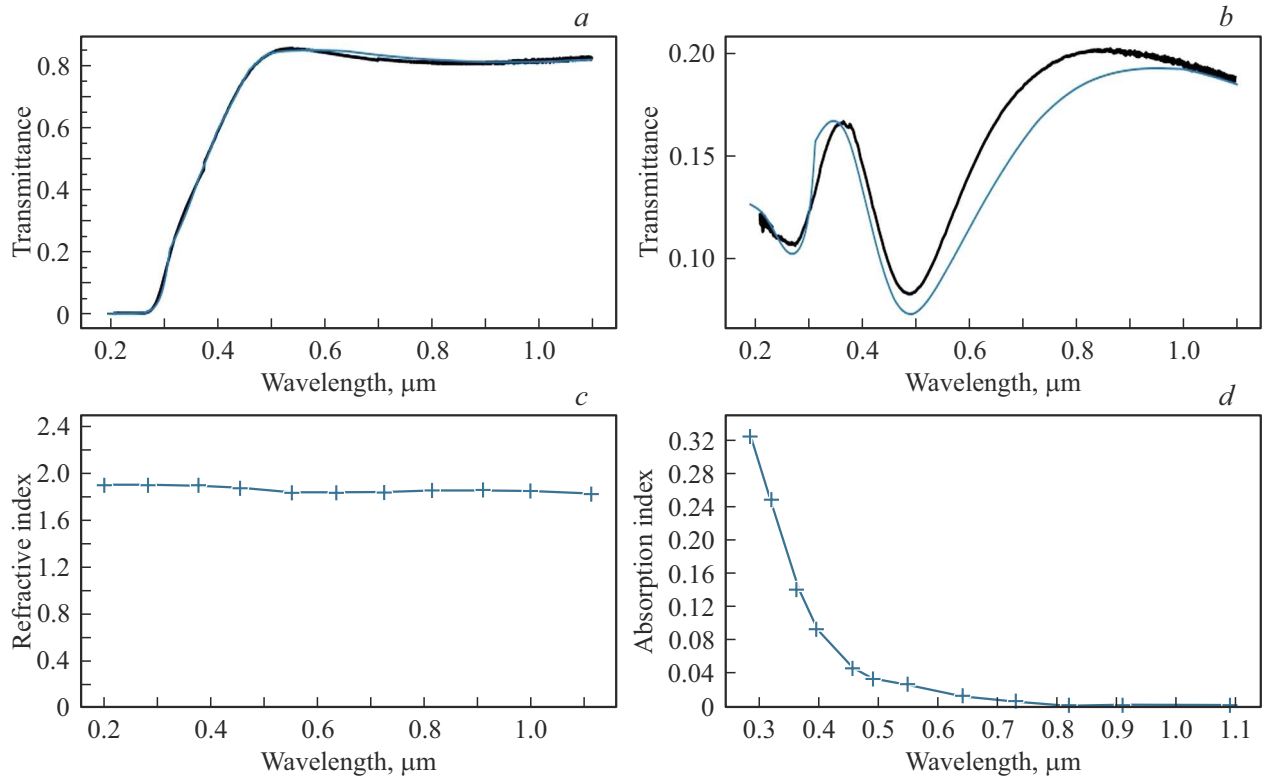

Figure 4. Example of modeling the transmittance (a) and reflection (b) spectra of GeO_x films after annealing at 280 °C: black curves — experimental data, blue curves — simulation data and calculation of dispersion curves for refractive index $n(c)$ and absorption index $k(d)$. The blue crosses were set manually so as to achieve the best match between the experimental and calculated transmittance and reflection spectra, while the values of n and k between the crosses were approximated linearly by the program.

To study the optical absorption edge, the transmittance and reflection spectra of GeO_x films were recorded before and after annealing (Figures 2 and 3). Interference is observed in all spectra in the wavelength region where absorption is weak. The drastic drop in transmittance at wavelengths less than $0.3\,\mu$m is explained by the light absorption in the glass substrate. The presence of interference makes it impossible to accurately determine the absorption edge in GeO_x films. To quantify the absorption and refractive index, the transmission and reflection spectra of GeO_x films were approximated using the program mentioned in „Experimental method“ section.

Figure 4 shows an example of approximated experimental transmittance and reflection spectra of GeO_x films after annealing at a temperature of 280 °C. In the modeling process, the refractive index (n) and absorption coefficient (k), as well as the film thickness were selected so as to achieve the coincidence of experimental and calculated transmittance and reflection spectra. As a result, dispersion curves were obtained for the optical constants n and k.

From the dependence of the absorption index (k) on the wavelength (λ), the spectral dependence of the absorption coefficient (α) can be found using formula $\alpha(\mathrm{cm}^{-1}) = 4\pi \cdot 10^4 \cdot k/\lambda\,(\mu\mathrm{m})$. The data were later used to calculate the optical gap using Tauc model. There is no translational symmetry in amorphous materials, which is why energy regions with high and low density of states appear. Intrinsic absorption is determined by the density of states, and the absorption edge is determined by a dip in the density of states. The absorption process does not require the participation of phonons, because the quasi-momentum conservation law does not apply here. To find the absorption edge, we may use the equation [19,20]:

$$\alpha = B \cdot (E_{\mathrm{ph}} - E_{\mathrm{opt}})^2 / E_{\mathrm{ph}},$$

where B — is a constant, E_{ph} — is a photon energy, E_{opt} — is an optical gap. If we plot $(\alpha E_{\mathrm{ph}})^{1/2}$ versus photon energy, then by extrapolating the linear part of the graph to the abscissa axis, we obtain the optical gap (E_{opt}) of GeO_x film. The dotted line in Figure 5 shows an example of graph extrapolation for the original GeO_x film. The intrinsic absorption edge of the germanium monoxide film before annealing was 2.7 eV. Similarly, E_{opt} was determined at different annealing temperatures of the film. It can be seen from Figure 5 that absorption is also present when the photon energy is less than E_{opt}, which is due to the presence of so-called Urbach „tails“ at the edge of the density of states gap [21]. As the annealing temperature rises, E_{opt} shifts towards lower energies (up to 1.23 eV). This is because of the non-oxygen-bound Ge in the film volume in the form of nanoclusters formed due

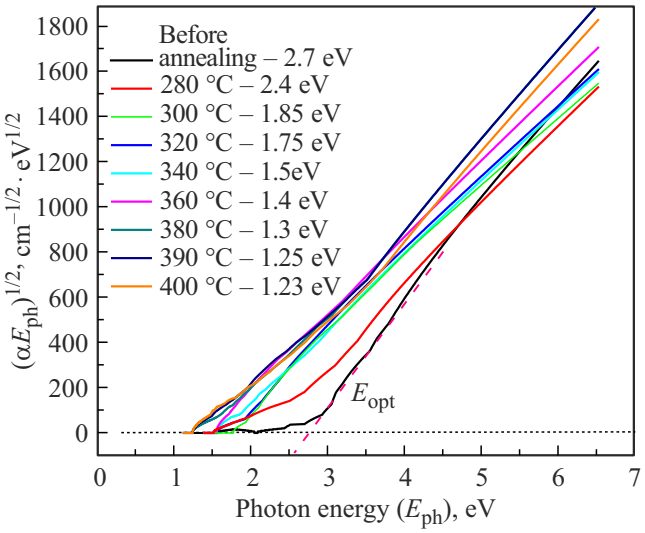

Figure 5. Evolution of the intrinsic absorption edge of GeO_x film before and after a series of annealing for 2 min.

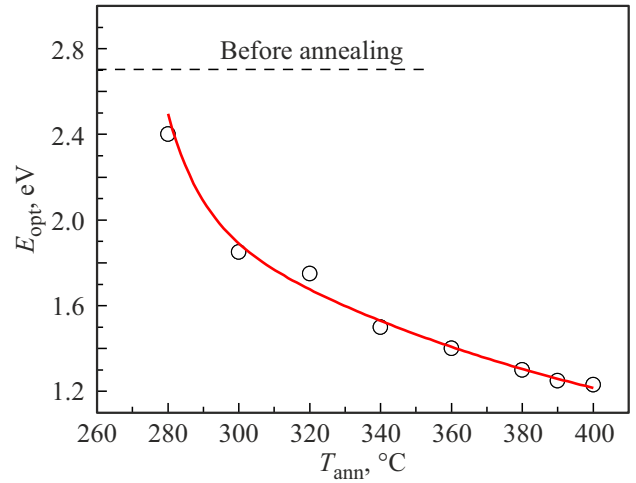

Figure 6. Change in the size of the optical gap (E_{opt}) of GeO_x film depending on the annealing temperature (T_{ann}).

to the disproportionation of GeO_x, as well as their growth, which is proved by RS spectroscopy data. It should be stressed that if the GeO_x film had been oxidized during annealing, then E_{opt}, on the contrary, would have shifted towards higher energies [22]. The optical gap for $GeO_{1.04}$ film turned out to be somewhat larger that described in the literature (2.4–2.5 eV) [6,9,23]. Obviously, this value depends on the composition, thickness, and structure of germanium monoxide film. Figure 6 shows that the optical gap (E_{opt}) for $GeO_{1.04}$ film declines exponentially depending on the annealing temperature (T_{ann}). Thus, using annealing, it is possible to control the edge of the intrinsic absorption of GeO_x films by varying the depth of disproportionation and obtaining structures with the required optical characteristics.

4. Conclusion

According to RS spectroscopy data, the disproportionation process begins in $GeO_{1.04}$ film with a thickness of $\sim 150-200$ nm at an annealing temperature of 280 °C. It was found that the onset temperature of crystallization process of Ge clusters (380 °C) in the studied film is lower than described in the literature. The dispersion dependences for the refractive and absorption indexes of GeO_x films before and after a series of annealing are found from the analysis of transmittance and absorption spectra in the spectral range $0.19-1.1\,\mu$m. The intrinsic absorption edge for $GeO_{1.04}$ film was found equal 2.7 eV. It has been established that annealing leads to a long-wavelength shift of the absorption edge, which is associated with the appearance and increase in the size of Ge nanoclusters.

Acknowledgments

The authors are grateful to the Center for Collective Use „VTAN“ Novosibirsk State University, for providing the equipment for recording the Raman spectra.

Funding

The films were prepared and heat-treated within the framework of the state assignment No FWES-2024-0002. The work on recording and analyzing the transmittance and reflection spectra of GeO_x films on glass was carried out as part of the state assignment No FWGW-2025-0014. The RS spectra of GeO_x films were registered as part of the state assignment No FWGW-2025-0023.

Conflict of interest

The authors declare no conflict of interest.

References

[1] A. Choudhury, A. Dalal, S.M. Manohar Dhar Dwivedi, A. Ghosh, N. Halder, S. Das, A. Mondal. Mater. Res. Bull. **142**, 111397 (2021). https://doi.org/10.1016/j.materresbull.2021.111397
[2] A. Chiasera, C. Macchi, S. Mariazzi, S. Valligatla, L. Lunelli, C. Pederzolli, D.N. Rao, A. Somoza, R.S. Brusa, M. Ferrari. Opt. Mater. Express **3**, *9*, 1561 (2013). https://doi.org/10.1364/OME.3.001561
[3] V.G. Dyskin, M.U. Dzhanklych. Appl. Solar Energy **57**, 252 (2021). https://doi.org/10.3103/s0003701x2103004x.
[4] V.F. Zinchenko, V.P. Sobol, I.R. Magunov, O.V. Mozgova. Voprosy khimii I khimicheskoi tekhnologii **6**, 29 (2018). https://doi.org/10.32434/0321-4095-2018-121-6-29-33
[5] K.N. Astankova, A.N. Aksenov, E.B. Gorokhov, I.A. Azarov, D.V. Marin, V.A. Volodin. Proc. Int. Symp. „Nanostructures: Physics and Technology“ (Ekaterinburg, Russia, 2011) p. 87.
[6] F.A. Nazarenkov, N.A. Rastrenenko. Optika i spektroskopiya **46**, *5*, 1013 (1979) (in Russian).

[7] E.B. Gorokhov, V.A. Volodin, D.V. Marin, D.A. Orekhov, A.G. Cherkov, A.K. Gutakovsky, V.A. Shvets, A.G. Borisov, M.D. Yefremov. FTP **39**, *10*, 1210 (2005) (in Russian).
[8] K.N. Astankova, E.B. Gorokhov, V.A. Volodin, D.V. Marin, I.A. Azarov, A.V. Latyshev. RN **11**, *5–6*, 59 (2016) (in Russian).
[9] G. Hamoud, A. Samus, A. Matsynin, S. Komogortsev, V. Zhandun, I. Prosvirin, K. Astankova, I. Azarov, P. Geydt, I. Milekhin, V. Volodin. Thin Solid Films **836**, 140869 (2026). https://doi.org/10.1016/j.tsf.2026.140869
[10] M. Wihl, M. Cardona, J. Tauc. J. Non-Cryst. Solids **8–10**, 172 (1972)
[11] D. Arsova, Ya. Bulmetis, K.Raptis, V. Pamukchieva, E. Skordeva. FTP **39**, *8*, 995 (2005) (in Russian). https://doi.org/10.1134/1.2010693
[12] J. Schroeder, W. Wu, J.L. Apkarian, M. Lee, L.-G. Hwa, C.T. Moynihan. J. Non-Cryst. Solids **349**, 88 (2004). https://doi:10.1016/j.jnoncrysol.2004.08.265
[13] J.H. Parker, D.W. Feldman, M. Ashkin. Phys. Rev. **155**, *3*, 712 (1967)
[14] V.A. Volodin, D.V. Marin, V.A. Sachkov, E.B. Gorokhov, H. Rinnet, M. Vergnat. JETP **118**, *1*, 65 (2014). https://doi.org/10.1134/S1063776114010208
[15] K. Vijayarangamuthu, S. Rath, D. Kabiraj, D.K. Avasthi, P.K. Kulriya, V.N. Singh, B.R. Mehta. J. Vac. Sci. Technol. A **27**, 731 (2009). http://dx.doi.org/10.1116/1.3155402
[16] F. Zhang, V.A. Volodin, K.N. Astankova, G.N. Kamaev, I.A. Azarov, I.P. Prosvirin, M. Vergnat. Results in Chem. **4**, 100461 (2022). https://doi.org/10.1016/j.rechem.2022.100461
[17] Yu. Chen, V.A. Volodin. Abstracts of reports of the School of Young Scientists „Physics and Technology of Quantum Systems“ (Novosibirsk, Russia, 2024) p. 50-51.
[18] K.N. Astankova, N.A. Kislukhin, I.A. Azarov, I.P. Prosvirin, V.A. Volodin. FTT **66**, *9*, 1585 (2024) (in Russian). http://dx.doi.org/10.61011/FTT.2024.09.58784.181
[19] B.P. Rai. Phys. Status Solidi A **100**, K189 (1987).
[20] J. Tauc, R. Grigorovici, A. Vanou. Phys. Status Solidi **15**, 627 (1966).
[21] F. Urbach. Phys. Rev. **92**, 1324 (1953)
[22] J. Beynon, M.M.A,G. El-Samanoudy, S.K.J. Al-Ani. J. Mater. Sci. Lett. **8**, 786 (1988).
[23] E.B. Gorokhov, T. Easwarakhantan, D.V. Marin, V.A. Volodin, K.N. Astankova, I.A. Azarov, M. Vergnat. Proc. Int. Symp. „*Nanostructures: Physics and Technology*“ (St. Petersburg, Russia, 2010) p. 329.

Translated by T.Zorina